151 IMPROVING THE ACCURACY OF NEAR-SURFACE 3-D RADAR REFRACTIVITY RETRIEVALS

Ya-Chien Feng* and Frédéric Fabry
McGill University, Montreal, Quebec, Canada

1. CHALLENGE AND MOTIVATION

The radar refractivity (N) retrieval technique developed by Fabry et al. (1997) provides insight on high-resolution near-surface moisture, which are considered important to pursuing knowledge of convective and boundary layer processes. For further quantitative application, such as assimilating refractivity into numerical models, or to implement this retrieval technique to radar networks, there remains some unsolved data quality problems that must be revisited and improved.

1.1 *Radar refractivity (N) and moisture*

The time that electromagnetic waves travel back and forth between the radar and the fixed target at range R is affected by the varied refractive index n along its propagating path. Refractivity is a function of pressure (P), temperature (T), and water vapor pressure (e). In addition, N is more sensitive to e change. At microwave frequencies, the empirical approximation of refractivity is (Smith and Weintraub 1953):

$$N = (n-1)\times 10^6 = 77.6\frac{P}{T} + 373000\frac{e}{T^2} \qquad (1).$$

The path-averaged refractivity (N) variation can be derived from the radar measured phase difference ($\Delta\phi$) of a stationary ground target between two time steps at time t and at a reference time t_{ref}:

$$\Delta\phi = \phi(t) - \phi(t_{ref}) \qquad (2)$$
$$= \frac{4\pi f}{c}\int_0^R [n(r',t) - n(r',t_{ref})]dr'.$$

, where f is the radar frequency, and c is the light speed in the vacuum.

1.2 *Revisiting the Fabry et al. (1997) assumptions*

The crude assumptions (Fabry et al. 1997) that were originally made to obtain a 2-D refractivity field are as follows: (1) Selected point targets are rigorously stationary on a flat Earth. Heights of selected targets are all aligned with the radar antenna height. (2) The vertical profile of refractivity index (dn/dh) is zero everywhere. Yet, these conditions are not always fulfilled in reality. These ideal assumptions were made because the heights of targets and refractivity profile (dn/dh) are unknown and earth curvature makes beam path more complicated. Real targets are at various heights, especially on hilly terrain or in an urban area. Besides, vertical variation of refractivity (dn/dh) varies diurnally (Park and Fabry, 2011) and changes significantly in those weathers we are interested in.

1.3 *Problems: noisy Δϕ and N bias*

The variability of target heights differences combined with the change in the profile of refractivity (dn/dh) introduces noisiness in phase difference (Fig. 1) and results in spatial and temporal biases of the retrieved refractivity. An example of the noisy phase difference ($\Delta\phi = \phi_{12UTC} - \phi_{00UTC}$) obtained under large changes of dn/dh is shown in Figure 1. The noisy phase differences ($\Delta\phi$) lead to difficulties in estimating the small-area radial gradients of phase differences and phase de-aliasing, which lower the quality of refractivity retrieval. In the post-processing, the noisy phase differences ($\Delta\phi$) are smoothed by either a pyramidal weighting function over a 4-km by 4-km or least square fitting (Fabry 2004; Nicol and Illingworth 2013). Nonetheless, the smoothing process still introduces biases on retrieved refractivity, which contain the unequal weighted information of dn/dh, and reduces the spatial resolution of the

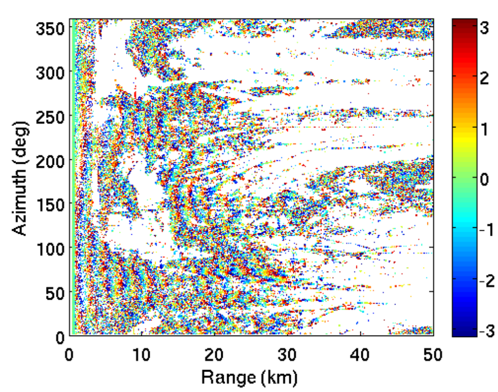

Fig. 1: The phase difference between two time-steps ($\Delta\phi = \phi_{12UTC} - \phi_{00UTC}$) in radians along the range (x-axis, in 125-m range gates) and the azimuth (y-axis, zero degrees is north).

* Corresponding author address: Ya-Chien Feng, McGill Univ., Dept. of Atmospheric and Oceanic Sciences, Montreal, QC, CANADA, H3A2K6; e-mail: ya-chien.feng@mail.mcgill.ca

data. Furthermore, when comparing refractivity measured by the radar and several instruments in the boundary layer, there are local and temporal discrepancies (Fabry 2006). Local errors may occur due to the variability of the heights of ground targets; temporal errors over the whole domain tend to happen during certain time periods, such as nighttime.

1.4 *Goal*

Accurate refractivity retrievals and the knowledge of observation bias are critical for quantitative applications, such as data assimilation into numerical weather models and short-term forecasting. Therefore, we quantify and try to solve the challenges of noisy phases and biases of refractivity retrieval associated with the vertical gradient of refractivity (d*n*/d*h*) and with target height. In the end, we expect to obtain a more accurate near-surface 3-D refractivity field, which consists of a 2-D horizontal refractivity map at given representative height and more reliable d*n*/d*h* information.

2. QUANTIFYING THE PROBLEMS

2.1 *The $\Delta\phi$ noisiness*

The observed phase is affected by the horizontal and vertical variation of refractivity along its beam path (Eq. 2). The range *R* of a one-way beam path travelling from the radar to the target is associated with the propagation condition (d*n*/d*h*) and the height of the target (H_T). Park and Fabry (2010) developed a simulator to explore the observed noisy phase difference ($\Delta\phi$) by considering the temporal change of vertical variation of refractivity (d*n*/d*h*) and the different target heights. Here, we separate range (*R*) into three terms: the arc distance (*D*) to the target at radar height (H_R), the range variation (ΔR_1) related to the height difference ($H_T - H_R$) while d*n*/d*h*= -157 ppm km^{-1}, and the range variation (ΔR_2) related to the variation of propagation condition d*n*/d*h*

$$R = D + \Delta R_1\left(D, H_T - H_R, \frac{dn}{dh_{-157}}\right) + \Delta R_2\left(D, \frac{dn}{dh} - \frac{dn}{dh_{-157}}\right) \quad (3)$$

When the antenna elevation is zero degrees and d*n*/d*h* is -157 ppm km^{-1}, the radar beam path is parallel to the earth curvature. The value of ΔR_1 can reach tens centimeters while ΔR_2 is typically a few centimeters.

Then, we rewrite the phase difference ($\Delta\phi$) equation (Park and Fabry, 2010) by substituting the range (*R, Eq.3*) and neglecting small terms of phase difference ($\Delta\phi$ < 1°) from scale analysis:

$$\Delta\phi = \frac{4\pi f}{c}\left[\begin{array}{c} D\left[\overline{n(t)} - \overline{n(t_{ref})}\right] + \overline{n(t_{ref})}\Delta R_2 \\ + \dfrac{D(H_T - H_R)}{2}\left[\left(\dfrac{dn}{dh}\right) - \left(\dfrac{dn}{dh}\right)_{t_{ref}}\right] \\ -D^3\left\{\left(\dfrac{dn}{dh}\right)\left[\dfrac{1 + (E_r + H_R)\left(\dfrac{dn}{dh}\right)}{12(E_r + H_R)}\right] - \left(\dfrac{dn}{dh}\right)_{t_{ref}}\left[\dfrac{1 + (E_r + H_R)\left(\dfrac{dn}{dh}\right)_{t_{ref}}}{12(E_r + H_R)}\right]\right\} \end{array}\right] \quad (4)$$

with E_r being the radius of earth, and H_T and H_R the heights of target and radar above sea level. The range (*R*) is replaced by distance (*D*) and there is an additional term, $\overline{n(t_{ref})}\Delta R_2$, which is due to the range variation associated with the change of d*n*/d*h*.

A horizontal refractivity map on the surface should be obtained only from the $D\left[\overline{n(t)} - \overline{n(t_{ref})}\right]$ term; other terms result in biases in 2-D refractivity retrieval. The phase difference ($\Delta\phi$) of a ground target is related to effects in Eq. 4: (i) the radial (horizontal) change of refractivity (left-hand side of 1st row), (ii) the target height alignment with respect to the radar associated with d*n*/d*h* (2nd row), and (iii) the ray curvature relative to the curvature of earth (right-hand side of 1st row and 3rd row). Once the height of target and the d*n*/d*h* are known, we can obtain a $\Delta\phi$ field only related to the horizontal variation of refractivity at a given height.

(a)

(b)

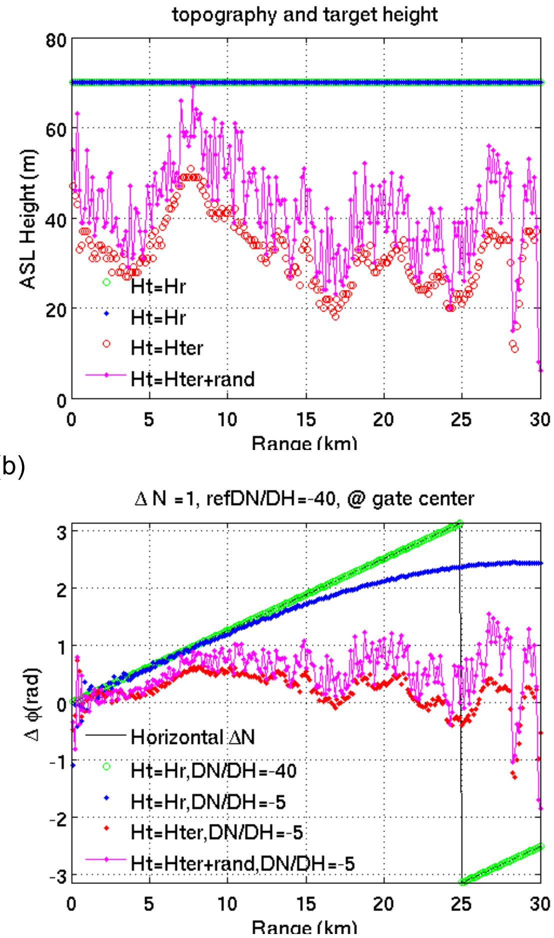

Fig. 2: (a) Height variation of targets with range. The red dots represent the topography; the magenta line shows the random variability of target heights within 20m above the terrain. (b) When horizontal refractivity change is 1 unit, the phase difference varies with the range. The black line shows the Δϕ caused only by horizontal ΔN change. The green line is $\Delta\phi$ when under no dn/dh change and target height alignment, therefore it overlaps with the black line. When dn/dh changes, $\Delta\phi$ varies with differnet target height distribution shown in blue ($H_T = H_R$), red ($H_T = H_{terrain}$), and magneta ($H_T = H_{terrain+random\ target\ height}$) lines.

The measured noisiness and bias of the phase difference ($\Delta\phi$) of targets at different heights is simulated based on Eq. 4 and shown in Figure 2. Under constant horizontal refractivity gradient (ΔN=1 unit), the phase difference increases linearly with range (Fig. 2b, black line). If dn/dh does not change and target height is aligned with radar height, the radial phase difference (green dot) is identical to what would be expected from the specified change in N. However, when dn/dh changes but target heights are similar, there is an increasing discrepancy associated with the change in the radar beam trajectory caused by propagation condition. Furthermore, for targets at terrain height (red line in Fig. 2a) and at random representative heights (magenta line in Fig. 2a), the corresponding phase differences (red and magenta lines in Fig. 2b) show both the bias and noisiness. During the type of weather phenomena we are particularly interested in, such as a moisture boundary with significant dn/dh variation, the bias of refractivity becomes larger and the phase difference is more difficult to decipher. The measured phases are affected by the 3-D refractivity variation of dn/dh along the path. The smoothing process does not really solve the problem physically and the biases remain. Both the 'noisy' and 'biased' phase difference field lowers the accuracy of refractivity estimation. In addition, the phase difference is more sensitive (noisier) for short-wavelength radars and far ranges.

2.2 *N bias*

The bias of refractivity retrieval (N_{bias}) is examined and quantified as $(c/4\pi f)*(\Delta\phi/D)$ based on Eq. (2), where $\Delta\phi$ is associated with the propagation condition (Δ(dn/dh)) and the target height differences ($H_T - H_R$). Here, the $(dn/dh)_{ref}$ is assumed as -40 ppm km^{-1}. We discuss the bias in two aspects; effects of trajectory (propagation) and of targets' height (Fig. 3).

***The refractivity bias due to the trajectory effect, N_{bias} (D, dn/dh)**:*

This refractivity bias is calculated from the phase difference associated with trajectory variation, which consists of the range variations due to dn/dh (the additional term on the first line of Eq. 4) and the radar beam curvature relative to the earth curvature (the 3rd line of Eq. 4). This refractivity bias increases with dn/dh change and distance to the target, as shown in Figure 3a. For instance, when dn/dh varies from -40 ppm km^{-1} (dn/dh at the reference state) to -120 ppm km^{-1}, the refractivity error of the target at 30 km away from the radar is about 0.5 N-unit. Moreover, this N bias is not linearly related to Δ(dn/dh) and depends on $(dn/dh)_{ref}$, which is required to be known at the calibration stage.

***The refractivity bias of target height effect, N_{bias} (ΔH, dn/dh)**:*

This N_{bias} is calculated from the 2nd line in Eq. (4) and is proportional to the height difference ($\Delta H = H_T - H_R$) between the radar and targets as well as the dn/dh variation (Fig.

2b), but independent on the target's position. The magnitude of this bias of the height effect is larger than the bias of trajectory effect. This height difference effect also explains the notable discrepancy of refractivity measured by the radar and the surface station when d*n*/d*h* changes a lot, such as during the change from day to night. In addition, this effect also shows that the local noisiness of phase difference is caused by neighboring targets having uneven heights. The noisy phase affects the diagnosis of radial phase difference gradient and leads to local noisiness in the refractivity retrieval.

(a)

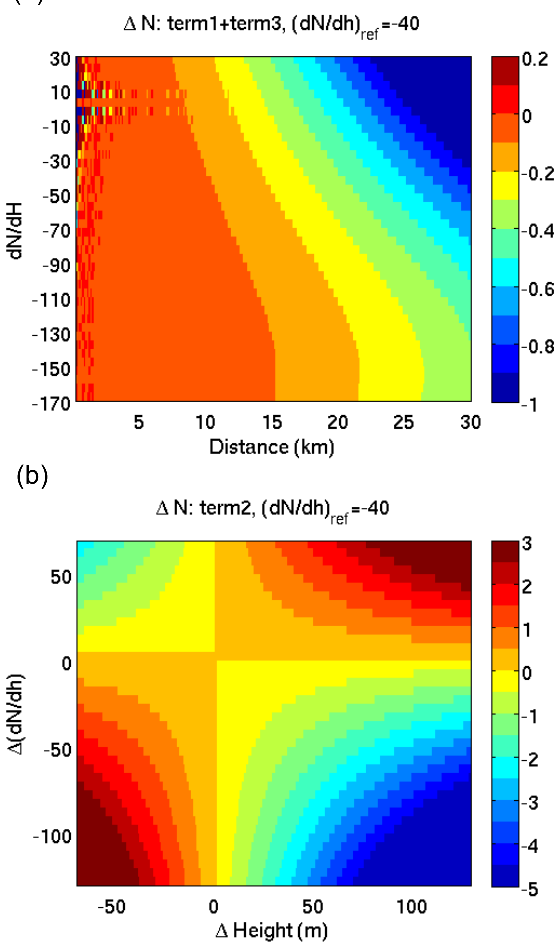

Fig. 3: (a) Refractivity bias, N_{bias} (*D*, d*n*/d*h*), related to the trajectory effect. This bias changes with the distance to targets (x-axis) and the atmospheric d*n*/d*h* condition (y-axis, unit of ppm km^{-1}). The d*n*/dh_{ref} is -40 ppm km^{-1}. (b) Refractivity bias, N_{bias} (ΔH, Δd*n*/d*h*), related to the target height effect. This bias is proportional to the height difference between targets and the radar (ΔH , x-axis) and the atmospheric d*n*/d*h* condition (Δd*n*/d*h*, y-axis, unit of ppm km^{-1}).

To summarize, in order to improve the refractivity fields, new approaches must be developed to estimate the representative height of the target and d*n*/d*h* by using existing and additional data. Consequently, noisiness of the phase difference will be expectedly reduced and the quality of 2-D refractivity maps at given height will be improved. In the end, a refractivity map at a given altitude will be utilized for characterizing the near-surface moisture boundary evolution or being assimilated to a short-term forecasting model to improve the initial condition of moisture.

3. LET'S SOLVE THE PROBLEMS! (POSSIBLE SOLUTIONS)

Additional dual-polarization data at multiple low elevation angles are collected to enhance the knowledge of the ground targets and improve the quality of returned phase used for retrieving refractivity. Both the phase and power of ground targets are affected by the evolving atmospheric conditions. For example, observed power and the phase of a fixed ground target, a power pole, are shown in Fig. 4 as a function of antenna elevation.

3.1 *Benefits from returned powers – Estimate target height and dn/dh*

The basic concept of using power variation at successive antenna elevations (*ele*) is based on the assumption of a known radar antenna pattern (assumed to be Gaussian here) and the point target. The radar beam pattern is convolved with the point target at successive antenna scanning elevations (*ele*); the returned power versus the antenna elevations should be the same shape as the radar beam pattern. The received power P(*ele*) of this target at the successive antenna elevations (*ele*) is a Gaussian-shaped distribution and can be written as:

$$P(ele) = 10log_{10}\left[\frac{\frac{1}{\sigma\sqrt{2\pi}}\exp\left(\frac{-(ele-\theta)^2}{2\sigma^2}\right)}{P_0}\right] \quad (5)$$

σ is the standard deviation of the Gaussian distribution and can be obtained from the 6-dB beamwidth, which is equal to $2\sigma\sqrt{2ln4}$. P_0 is the reference maximum power when the center of the main beam exactly hit the target (*ele* = θ). The representative elevation (θ) of a target at distance (*D*) from the radar is constant under given d*n*/d*h* and can be expressed in a function:

$$\theta\left(D, H_T, \frac{dn}{dh}\right) = \tan^{-1}\left[\frac{1}{\sin\left(\frac{D}{a_e}\right)} * \left(\cos\left(\frac{D}{a_e}\right) - \frac{a_e}{H_T + a_e - H_R}\right)\right] \quad (6)$$

$$a_e = \frac{1}{1 + E_r(\frac{dn}{dh})} \quad (7)$$

E_r is the radius of the earth, and a_e is the effective radius of the earth associated with d*n*/d*h* variation.

(a)

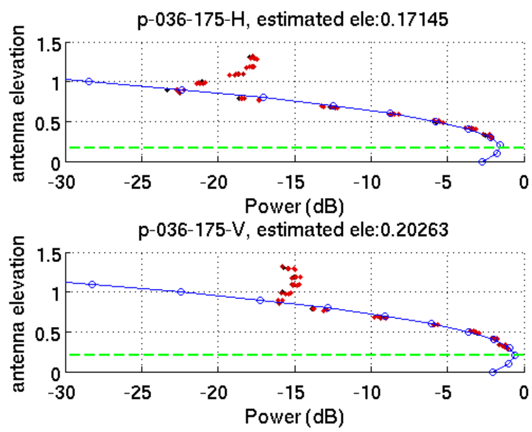

(b)

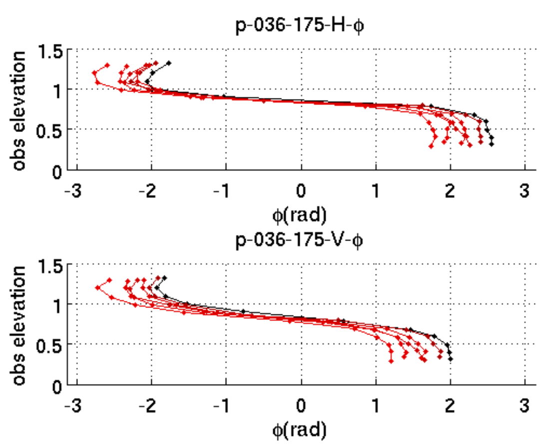

Fig. 4: (a) The returned power of a fixed target (at 36° azimuth, 175th gate) at successive antenna elevations from 0.3° to 1.3°. Reddish dots represent different scans within 30 minutes. The blue line is fitting a Gaussian antenna gain curve to the power variation versus the elevations. The upper panel is for horizontal polarization; and the lower panel is for the vertical polarization. (b) The phases at successive antenna elevations.

Estimate target height

Thus, a new method is proposed to obtain the representative target height (H_T) and atmospheric d*n*/d*h* condition by fitting the received powers at successive elevations with a Gaussian distribution function (Fig. 4a, blue lines). The representative elevation (θ) of the point target is detected as the antenna elevation with peak of the returned power (Fig. 4a, green dash). As a consequence, we might estimate the representative height (H_T) of the target based on the following equation, which is rewritten from Doviak and Zrnic (1991),

$$H_T = ae\left[\frac{\cos(\theta)}{\cos(\theta + \frac{D}{a_e})} - 1\right] \quad (8)$$

The representative elevation (θ) is sensitive to the fitting algorithm and the 'θ' affects the result of height estimation significantly. A very accurate θ to the second digit point is required, but is difficult to be obtained especially for targets at far range. Taking a target at 30km for instance, the 0.1° difference of representative elevations leads to 50m differences in height. Another possible fitting method is fitting the first null of the antenna, where is usually the center of the transition of phase at increasing elevations.

Estimate dn/dh

Time series of representative elevation (θ) of a fixed target can illustrate the temporal variation of d*n*/d*h* based on Eq. (6). However, for operational radars, it is not practical to execute a routine scanning strategy with many low elevations. Hence, an alternative algorithm of only using two low elevations is developed. The representative elevation (θ) changes with d*n*/d*h*; but the returned power versus elevations remains the same Gaussian-shaped curve (Fig. 5a). As a result, there is a relation between power differences of two given elevations ($\Delta P = P_{0.3°} - P_{0.5°}$) and d*n*/d*h* (this term is included in θ):

$$\Delta P = P_{0.3°} - P_{0.5°} = 10log_{10}\exp\left(\frac{0.16 - 0.4\theta}{2\sigma^2}\right) \quad (9)$$

The d*n*/d*h* information can be extracted from the temporal variation of ΔP. Based on the Eq. (6) and (9), it shows a linear relation between d*N*/d*h* and power difference (Fig. 5b, upper panel). The more negative the d*N*/d*h*, the smaller the ΔP. Because the amount of ΔP is related to the properties of target, such as height, distance, etc, ΔP is not identical for different targets under the same dn/dh change. Thus, the ΔP is normalized to demonstrate the relative dN/dh change of a day (Fig. 5b, lower panel) as:

$$\frac{\left(\frac{dn}{dh}\right) - \left(\frac{dn}{dh}\right)_{min}}{\left(\frac{dn}{dh}\right)_{max} - \left(\frac{dn}{dh}\right)_{min}} = \frac{\Delta \mathrm{P} - \Delta \mathrm{P}_{min}}{\Delta \mathrm{P}_{max} - \Delta \mathrm{P}_{min}} \qquad (10)$$

Taking a real ground target as an example, the diurnal variation of the power of a target at 0.3° and 0.5° antenna elevations are shown in Figure 6a. During the nighttime (00 to 09UTC)

(a)

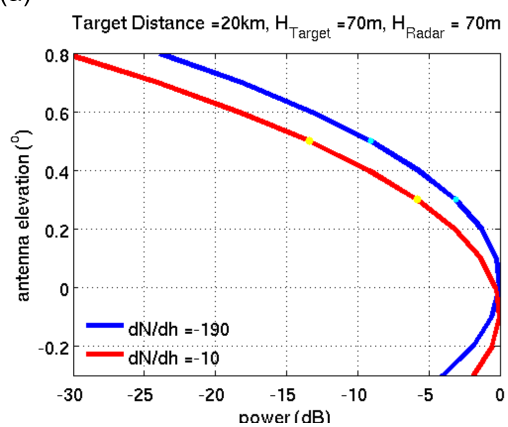

(b)

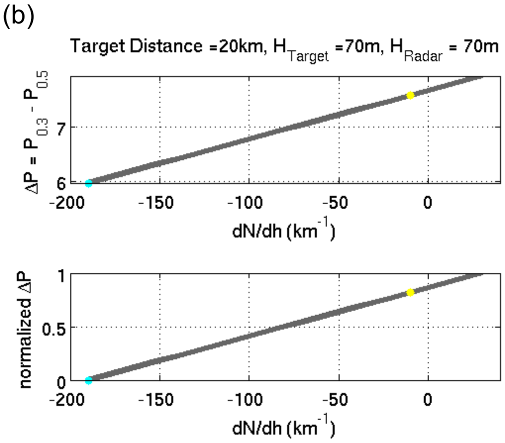

Fig. 5: (a) The returned power at successive antenna elevations under different dN/dh conditions simulated based on Eq.(5). The red line is when dN/dh = -10 ppm km^{-1}, and blue line is for dN/dh = -190 ppm km^{-1}. The dots show the selected antenna elevations. (b) Example of one target at 20km from radar and with same height as radar. Upper panel shows the simulation power differences of two given elevations ($\Delta P = P_{0.3°} - P_{0.5°}$) and different d$N$/d$h$ conditions. Lower panel shows the normalized power differences versus dN/dh.

with more negative dn/dh, the beam bends toward the ground and causes the power to increase at both elevations. Nonetheless, the difference of power at two elevations (Fig. 6b) shows the diurnal cycle as the expected qualitative variation of dn/dh. The temporal power difference is noisy and is smoothed by using a running average method (Fig. 6b, black line). The power difference is normalized shown in Fig. 6c. The estimated dn/dh trends from different targets show local consistency. In summary, powers at successive low elevations provide the representative target height and dn/dh, which are the key factors associated with the error of refractivity retrieval.

3.2 *Benefits of phases at dual-polarization: Target quality*

The phase variations at H- and V-polarizations of a 'point' ground target are expected to be identical and coherent under a given atmospheric condition. But in reality, for some real targets, they are not. Figure 7a shows the discrepancy of phase difference ($\Delta\phi$) at two polarizations, particularly during the large change of dn/dh in the night. Based on the second line of Eq. (4), the discrepancy of phase difference between the two polarizations should be proportional to the Δ(dn/dh) and height difference between two polarizations. This result reminds us to rethink the 'point' target assumption, because this discrepancy of phase might be the result of the different representative heights of H- and V-polarizations. In other words, they are 'extended' targets.

Moreover, when the discrepancy occurred in the nighttime, the power of the target abnormally decreases due to the anomalous propagation (Fig. 7b). This might imply the destructive interference of the extended or complex target during large dn/dh change. Therefore, the discrepancy of phase difference between two polarizations and the abnormal power variation could be used as a warning concerning the quality of the phase data at certain time periods.

4. Summary

Dual-polarization data at low elevations provides information on the vertical gradient of refractivity (dn/dh) and the representative target heights, which are the key factors that affect the quality of phase used for refractivity retrieval. Further validation of dn/dh and target heights will be examined, and the data processing flow to reducing noisiness of phase difference will be developed considering the additional information of d*n*/d*h* and target height (including terrain information and differential target height). After applying the information, the noisiness of phase difference for uneven target heights in the bumpy terrain area are expected to be reduced, which will increase the data horizontal resolution of the refractivity data. Ultimately, the height of the final output refractivity map will be defined either at a given height or following the terrain. A more accurate low-level 3-D refractivity (or the phase) and knowledge of retrieval errors are expected for further quantitative applications.

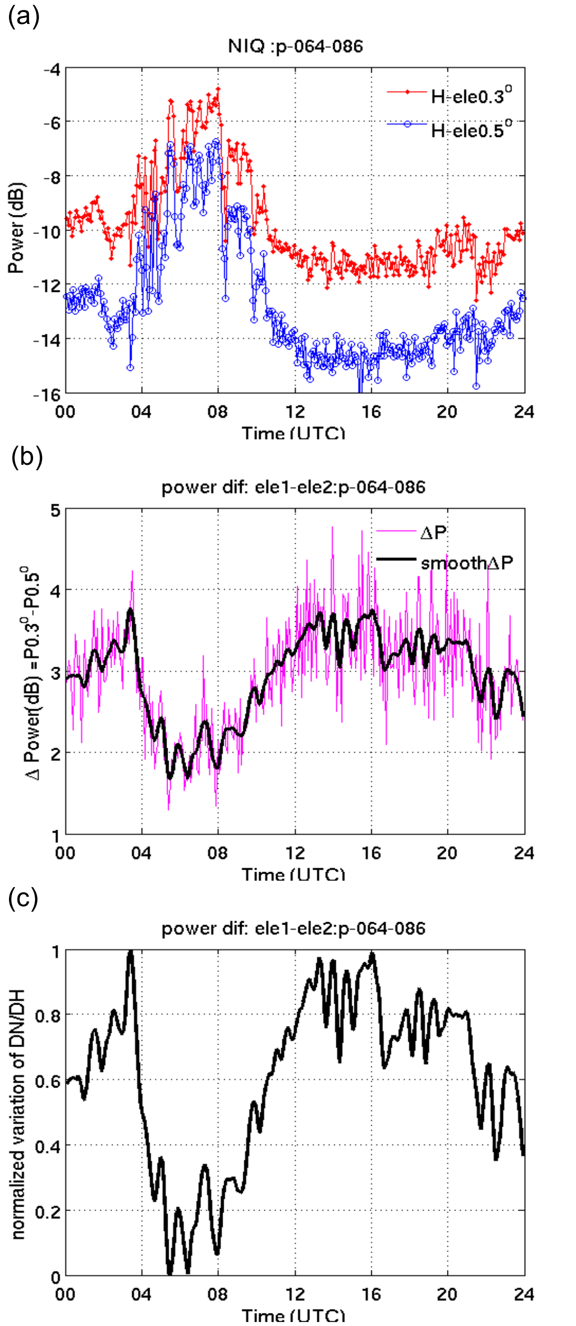

Fig. 6: (a) Time series of returned power from a point target at 0.3°(red) and 0.5° (blue) elevations. (b) The power difference between 0.3° and 0.5° elevations are shown in pink. The black line is the smoothed power difference. (c) The normalized d*n*/d*h* varies between 0 (dn/dh_{min}) to 1 (dn/dh_{max}) in a day. LST = UTC-4. Nighttime is from 00 to 09 UTC.

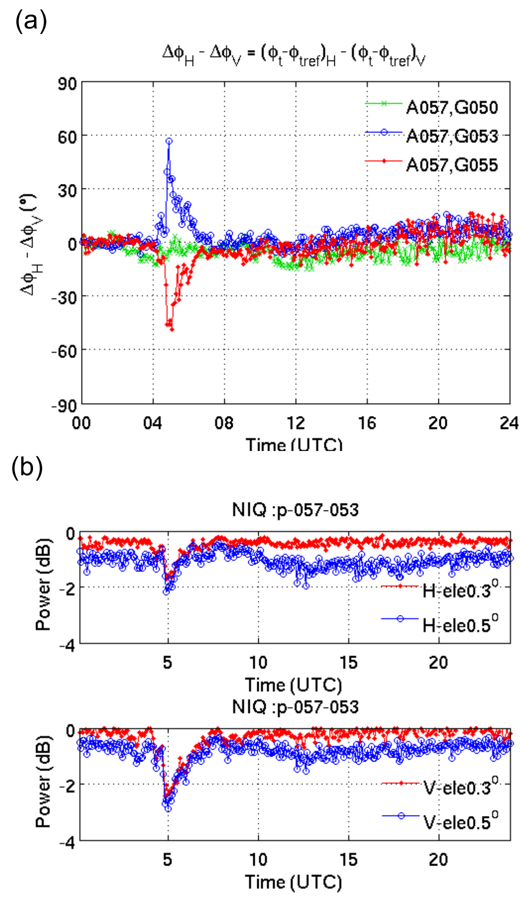

Fig. 7: (a) Time series of successive phases difference between two polarizations ($\Delta\phi_H - \Delta\phi_V = (\phi_t - \Delta\phi_{t-1})_H - (\phi_t - \Delta\phi_{t-1})_V$) for three nearby targets at same azimuth. Note the abnormal part in the night (03 -06 UTC). (b) Time series of returned power from one target at different polarization and elevations. The upper level is at horizontal polarization, the lower one s at vertical polarization.

Reference:

Doviak, R. J., and D. S. Zrnić, 1993: *Doppler Radar and Weather Observations*. 2nd ed. Academy Press, 562 pp.

Fabry, F., C. Frush, I. Zawadzki, and A. Kilambi, 1997: On the extraction of near-surface index of refraction using radar phase measurements from ground targets. *J. Atmos. Oceanic Technol.*, **14,** 978-987.

Fabry, F., 2004: Meteorological value of ground target measurements by radar. *J. Atmos. Oceanic Technol.*, **21,** 560-573.

——, 2006: The spatial variability of moisture in the boundary layer and its effect on convection initiation: Project-long characterization. *Mon. Wea. Rev.*, **134,** 79-91.

Nicol, J. C., and A. J. Illingworth, 2013: The effect of phase-correlated returns and spatial smoothing on the accuracy of radar refractivity retrievals. *J. Atmos. Oceanic Technol.*, **30,** 22-39.

Park, S., and F. Fabry, 2010: Simulation and interpretation of the phase data used by the radar refractivity retrieval algorithm. *J. Atmos. Oceanic Technol.*, **27,** 1286-1301.

——, 2011: Estimation of near-ground propagation conditions using radar ground echo coverage. *J. Atmos. Oceanic Technol.*, **28,** 165-180.

Smith, E. K., and S. Weintraub, 1953: The constants in the equation for atmospheric refractive index at radio frequencies. *Proceedings of the IRE*, **41,** 1035-1037.